ISSN 1063-7737, Astronomy Letters, 2021, Vol. 47, No. 12, pp. 863–871. © Pleiades Publishing, Inc., 2021.
Russian Text © The Author(s), 2021, published in Pis'ma v Astronomicheskii Zhurnal, 2021, Vol. 47, No. 12, pp. 900–908.

Kinematic Properties of the GAIA EDR3 Catalogue

A. S. Tsvetkov[1]*

[1] *St. Petersburg State University, St. Petersburg, 198504 Russia*

Received August 22, 2021; revised November 11, 2021; accepted December 4, 2021

Abstract—We have obtained a solution of the Ogorodnikov–Milne stellar-kinematics equations based on the material of the entire Gaia EDR3 star catalogue containing 1.8 billion objects. In view of the insufficient accuracy of individual trigonometric parallaxes, we have also obtained an analogous solution based on a sub-catalogue of selected 98 million stars for which the parallaxes are known with an accuracy better than 10%. We have performed a detailed analysis of these solutions as a function of stellar magnitude and distance.

DOI: 10.1134/S1063773721120057

Keywords: *Gaia, astrometry, space astrometry, stellar kinematics, Galactic structure.*

INTRODUCTION

The Gaia spacecraft continues its in-orbit operation; the final catalogue is planned to be published in the first half of 2022 (ESA, Gaia). Preliminary Data Release catalogues have already been published: DR1 and DR2. On December 3, 2020, the Gaia Early Data Release 3 (Gaia EDR3), an "early release of the final catalogue" (Gaia, EDR3), was published. The technique for its construction and details are presented in Gaia Collaboration (2021). Such a number of papers that it is impossible to give even briefly their names alone are devoted to these data.

The quality of individual parallaxes in Gaia EDR3 is still very far from the predicted one (more on this below). Therefore, we carried out a series of standard studies that had already been applied (Vityazev et al. 2017) to extensive catalogue of stars, such as NOMAD (Zacharias et al. 2004) containing 1.1 billion objects or PPMXL (Roeser et al. 2010) containing 910 million stars. These studies include the acquisition of various statistical data, a standard stellar-kinematics analysis, and an analysis using spherical harmonics (Vityazev and Tsvetkov 2014).

CATALOGUE ORGANIZATION

The input data of the EDR3 catalogue are accessible at the official Gaia site in the form of 3386 compressed files with a volume ∼200 MB each. After decompression, the file volume approximately doubles and is 400–450 MB. Thus, the total volume of the data being downloaded is ∼670 GB, while the decompressed data require storage with a volume ∼1.5 TB. The format of the files, CSV, is the text one, the entry fields for each star are separated by a comma. If some data are lacking (and this happens often), two commas follow in a row. Such an input data format is easily maintained by the FORTRAN language (Barteniev 2000).

Each row contains information 99 fields for one star. A detailed description of each field is given in Gaia (Chapter 13). The fields can be divided into the following categories:

- identifiers;
- astrometric parameters: the coordinates, proper motions, parallaxes, and their errors;
- correlations between parameters;
- the number and quality of astrometric observations (the largest group);
- photometry in three bands;
- radial velocities (from DR2);
- Galactic and ecliptic coordinates.

THE ACCURACY OF PARALLAXES

Highly accurate individual stellar parallaxes are the most important planned Gaia result. At present, the declared accuracy (0.01 mas) has not yet been achieved for most stars (Brown et al. 2021). There are data on the parallaxes in EDR3 for 1 467 744 818 stars, while 343 964 953 stars do not have these data. An

*E-mail: a.s.tsvetkov@inbox.ru

analysis of the parallaxes showed that there is a large fraction of stars for which the errors are tenths of mas or more. Only 500 million stars, i.e., approximately a third of the stars with data on the parallaxes, have an accuracy better than 0.2 mas. As a result, only 520 million stars have a relative parallax accuracy better than 50% and only 98 million stars have an accuracy better than 10%; 283 million stars have even negative parallaxes (which contradicts the geometrical meaning of the parallax). In this case, as a more detailed analysis shows, these parallaxes do not necessarily have large rms errors. This fact demonstrates that the work on the Gaia parallaxes requires a considerable effort and the establishment of an accurate parallax zero point.

Thus, the individual parallaxes should be used with great caution, although statistically, for large groups of stars, the averaged parallaxes give quite reliable results.

THE ACCURACY OF PROPER MOTIONS

All 1 811 709 771 stars, without exception, have data on the proper motions. The accuracies given in the catalogue have not yet achieved the planned ones in terms of random errors. Only 213 million stars and 406 million stars have a total proper motion accuracy better than 0.1 and 0.2 mas yr^{-1}, respectively. However, the relative accuracy of the proper motions is much better that that of the parallaxes, because the proper motions themselves are greater than the parallactic shifts. The total proper motion lies within the ranges from 2 and 8 mas yr^{-1} and from 0 to 10 mas yr^{-1} for 77 and 93% of the stars, respectively. Thus, almost half of the stars in the catalogue have a relative proper motion accuracy better than 10%. Such a high accuracy makes it possible to carry out any stellar-kinematics studies based on the analysis of stellar proper motions.

PHOTOMETRIC DATA

Gaia uses its own photometric system (Montegriffo et al. 2020). The "blue" component G_{BP} spans the range from the near ultraviolet to the red; the "red" component G_{RP} spans the range from the red to the infrared. This system differs from the UBV scale not only by different boundaries of the photometric bands, but also by their widths. The relationship of the Gaia photometric scale to other photometric systems will be established later (Riello et al. 2021).

The G magnitudes are available for almost all stars (absent only for 5 million stars), whereas G_{BP} and G_{RP} photometry is available for slightly more than 1.5 billion stars (absent for 270 million stars).

The catalogue gives the measured photon fluxes in three bands and their errors, while there are no errors of the magnitudes themselves, because the magnitudes are related nonlinearly to the measured flux (Gaia, Chapter 13).

KINEMATIC ANALYSIS OF STELLAR PROPER MOTIONS FROM THE FULL CATALOGUE WITHOUT USING INDIVIDUAL DISTANCES

The Gaia catalogue gives only the equatorial stellar proper motions $\mu_\alpha \cos\delta$ and μ_δ. It is nor difficult to convert them to the Galactic $\mu_l \cos b$ and μ_b that will be used in our studies.

As the main model we use the widely known Ogorodnikov–Milne model (Ogorodnikov 1965); a detailed form of the equations for this model is also presented in du Mont (1977) and Rybka (2004). In the model the stellar velocity field is represented by a linear expression:

$$\mathbf{V} = \mathbf{V}_0 + \mathbf{\Omega} \times \mathbf{r} + \mathbf{M}^+ \times \mathbf{r}, \qquad (1)$$

where $\mathbf{V}$ is the stellar velocity, $\mathbf{V}_0$ is the influence of the translational solar motion, $\mathbf{\Omega}$ is the angular velocity of rigid-body rotation of the stellar system, and $\mathbf{M}^+$ is the symmetric deformation tensor of the velocity field.

The model contains only 12 parameters. However, not all of them can be independently determined from the proper motions, and not all the parameters enter into the equations for the radial velocities:

$[U, V, W]$ are the components of the Sun's translational velocity vector $\mathbf{V}_0$ relative to the stars;

$[\omega_1, \omega_2, \omega_3]$ are the components of the angular velocity vector $\mathbf{\Omega}$;

$[M_{11}^+, M_{22}^+, M_{33}^+]$ are the parameters of the deformation tensor describing the contraction/extension along the principal axes of the Galactic coordinate system;

$[M_{12}^+, M_{13}^+, M_{23}^+]$ are the parameters of the tensor $\mathbf{M}^+$ describing the velocity field deformation in the principal plane and two planes perpendicular to it.

Projecting Eq. (1) onto the unit vectors of the Galactic coordinate system, for the proper motions we have

$$\begin{aligned} k\mu_l \cos b = {} & U/r \sin l - V/r \cos l \qquad (2) \\ & - \omega_1 \sin b \cos l - \omega_2 \sin b \sin l + \omega_3 \cos b \\ & + M_{12}^+ \cos b \cos 2l - M_{13}^+ \sin b \sin l \\ & + M_{23}^+ \sin b \cos l - \frac{1}{2} M_{11}^+ \cos b \sin 2l \\ & + \frac{1}{2} M_{22}^+ \cos b \sin 2l, \end{aligned}$$

Table 1. The components of the solar velocity and the angular velocity of rigid-body rotation, in km s^{-1} kpc^{-1}, derived from the simultaneous solution for stars with various G magnitudes

G	$U/\langle r\rangle$	$V/\langle r\rangle$	$W/\langle r\rangle$	ω_1	ω_2	ω_3
3	158.1 ± 44.5	294.2 ± 45.4	159.4 ± 42.5	45.6 ± 45.2	19.4 ± 45.7	-26.4 ± 42.3
4	184.9 ± 31.3	209.2 ± 32.0	128.1 ± 29.3	-59.5 ± 32.2	25.8 ± 32.6	3.6 ± 29.3
5	116.5 ± 10.6	181.0 ± 10.7	71.5 ± 9.9	-13.1 ± 10.8	13.2 ± 10.9	-21.1 ± 9.8
6	75.0 ± 4.9	132.3 ± 5.0	50.7 ± 4.5	6.1 ± 5.0	8.2 ± 5.1	-15.6 ± 4.5
7	59.6 ± 1.9	111.2 ± 1.9	38.4 ± 1.8	1.9 ± 1.9	-7.5 ± 2.0	-12.2 ± 1.8
8	44.8 ± 1.0	91.3 ± 1.0	30.4 ± 1.0	0.6 ± 1.0	-4.9 ± 1.0	-11.4 ± 1.0
9	35.0 ± 0.6	77.7 ± 0.6	25.2 ± 0.6	1.5 ± 0.6	-4.4 ± 0.6	-10.7 ± 0.6
10	30.1 ± 0.3	67.1 ± 0.3	19.5 ± 0.3	0.6 ± 0.3	-2.8 ± 0.3	-11.6 ± 0.3
11	24.9 ± 0.2	58.8 ± 0.2	15.9 ± 0.2	0.8 ± 0.2	-2.4 ± 0.2	-11.8 ± 0.2
12	20.6 ± 0.1	51.6 ± 0.1	13.1 ± 0.1	0.2 ± 0.1	-2.0 ± 0.1	-11.9 ± 0.1
13	17.3 ± 0.1	46.3 ± 0.1	10.7 ± 0.1	0.3 ± 0.1	-1.1 ± 0.1	-12.4 ± 0.1
14	14.9 ± 0.1	42.5 ± 0.1	8.8 ± 0.1	0.4 ± 0.1	-0.9 ± 0.1	-12.8 ± 0.1
15	12.7 ± 0.1	39.8 ± 0.1	7.3 ± 0.1	0.5 ± 0.1	-0.7 ± 0.1	-12.9 ± 0.1
16	10.9 ± 0.1	38.1 ± 0.1	6.3 ± 0.1	0.6 ± 0.1	-0.7 ± 0.1	-12.6 ± 0.1
17	9.63 ± 0.05	36.95 ± 0.05	5.51 ± 0.05	0.62 ± 0.05	-0.70 ± 0.05	-12.29 ± 0.05
18	8.37 ± 0.04	35.48 ± 0.04	4.92 ± 0.04	0.38 ± 0.04	-0.57 ± 0.04	-12.08 ± 0.04
19	7.15 ± 0.04	33.19 ± 0.04	4.36 ± 0.04	0.25 ± 0.04	-0.46 ± 0.04	-11.93 ± 0.04
20	6.48 ± 0.03	31.69 ± 0.03	4.15 ± 0.03	0.33 ± 0.03	-0.51 ± 0.03	-11.80 ± 0.03

Table 2. The components of the deformation tensor, in km s^{-1} kpc^{-1}, derived from the simultaneous solution for stars with various G magnitudes

G	M_{12}^{+}	M_{13}^{+}	M_{23}^{+}	M_{11}^{*}	X
3	-36.1 ± 55.2	18.3 ± 58.1	-126.9 ± 57.1	192.9 ± 110.8	1.1 ± 103.8
4	-1.8 ± 37.8	4.1 ± 41.5	28.3 ± 39.6	-127.3 ± 78.5	37.2 ± 74.8
5	15.1 ± 13.0	9.3 ± 13.7	2.1 ± 13.5	6.9 ± 25.9	-39.9 ± 25.1
6	25.2 ± 6.0	17.1 ± 6.4	-5.0 ± 6.3	1.3 ± 11.9	8.9 ± 11.6
7	14.6 ± 2.3	-3.3 ± 2.5	-3.4 ± 2.4	2.8 ± 4.6	-7.0 ± 4.4
8	15.2 ± 1.3	-2.3 ± 1.3	-2.9 ± 1.3	-3.0 ± 2.5	-2.1 ± 2.3
9	15.6 ± 0.8	-1.9 ± 0.8	-1.9 ± 0.8	-1.2 ± 1.6	1.6 ± 1.4
10	17.1 ± 0.4	-0.9 ± 0.4	-1.1 ± 0.4	-0.3 ± 0.9	-0.7 ± 0.7
11	15.9 ± 0.2	-0.5 ± 0.2	-1.3 ± 0.2	-1.3 ± 0.5	1.3 ± 0.4
12	15.2 ± 0.2	-0.5 ± 0.2	-0.4 ± 0.2	-1.2 ± 0.3	0.6 ± 0.3
13	14.3 ± 0.1	-0.1 ± 0.1	-0.1 ± 0.1	-1.4 ± 0.2	1.4 ± 0.2
14	13.3 ± 0.1	-0.3 ± 0.1	-0.3 ± 0.1	-1.1 ± 0.2	1.0 ± 0.1
15	12.7 ± 0.1	-0.4 ± 0.1	-0.4 ± 0.1	-0.9 ± 0.1	0.9 ± 0.1
16	12.1 ± 0.1	-0.3 ± 0.1	-0.5 ± 0.1	-0.3 ± 0.1	0.5 ± 0.1
17	11.4 ± 0.1	-0.1 ± 0.1	-0.4 ± 0.1	0.1 ± 0.1	0.3 ± 0.1
18	10.2 ± 0.1	0.1 ± 0.1	-0.1 ± 0.1	0.4 ± 0.1	0.4 ± 0.1
19	9.12 ± 0.05	0.18 ± 0.05	-0.02 ± 0.05	0.5 ± 0.1	0.6 ± 0.1
20	8.64 ± 0.04	0.12 ± 0.04	-0.15 ± 0.04	0.4 ± 0.1	0.6 ± 0.1

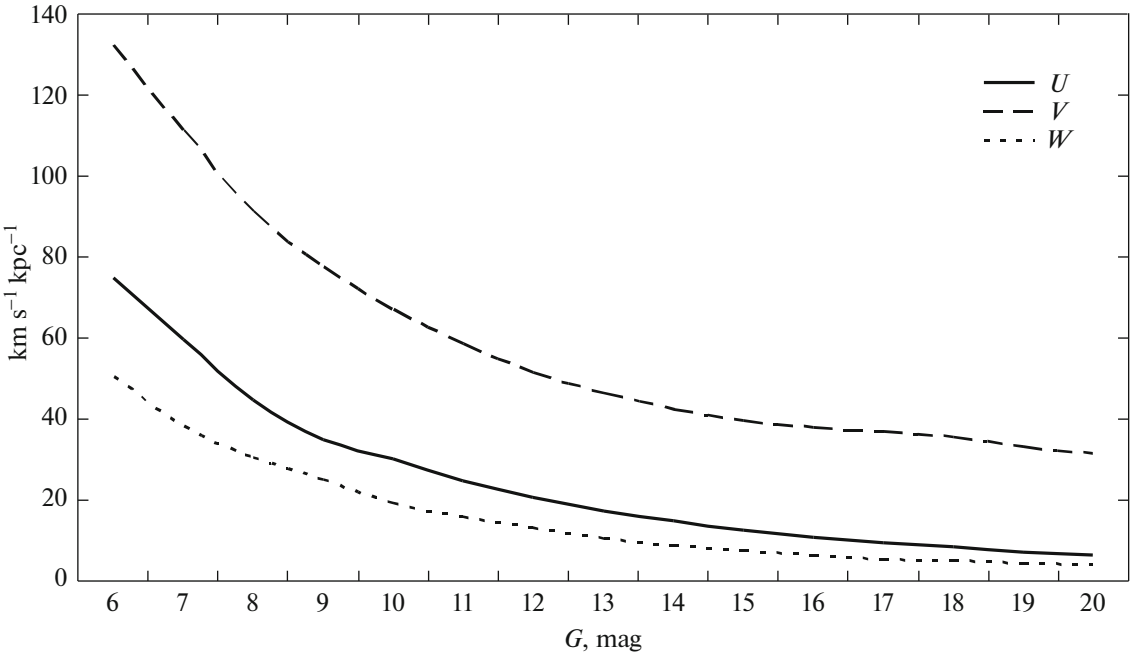

Fig. 1. Kinematic parameters of the solar motion $U/\langle r\rangle$, $V/\langle r\rangle$, $W/\langle r\rangle$ (km s^{-1} kpc^{-1}) versus magnitude.

$$k\mu_b = U/r\sin b\cos l + V/r\sin b\sin l - W/r\cos b + \omega_1\sin l - \omega_2\cos l - \frac{1}{2}M_{12}^{+}\sin 2b\sin 2l + M_{13}^{+}\cos 2b\cos l + M_{23}^{+}\cos 2b\sin l - \frac{1}{2}M_{11}^{+}\sin 2b\cos^2 l - \frac{1}{2}M_{22}^{+}\sin 2b\sin^2 l + \frac{1}{2}M_{33}^{+}\sin 2b. \quad (3)$$

In Eqs. (2) and (3) there is a linear relation among the coefficients M_{11}^{+}, M_{22}^{+}, and M_{33}^{+}. Therefore, when analyzing the proper motions, the authors usually introduce the substitutions $M_{11}^{*} = M_{11}^{+} - M_{22}^{+}$ and $M_{33}^{*} = M_{33}^{+} - M_{22}^{+}$ (du Mont 1977) or introduce the following quantity instead of M_{33}^{*} (Vityazev et al. 2018):

$$X = M_{33}^{+} - \frac{M_{11}^{+} + M_{22}^{+}}{2}. \quad (4)$$

In this case, Eqs. (2) and (3) are rewritten as

$$k\mu_l\cos b = U/r\sin l - V/r\cos l - \omega_1\sin b\cos l - \omega_2\sin b\sin l + \omega_3\cos b + M_{12}^{+}\cos b\cos 2l - M_{13}^{+}\sin b\sin l + M_{23}^{+}\sin b\cos l - \frac{1}{2}M_{11}^{*}\cos b\sin 2l, \quad (5)$$

$$k\mu_b = U/r\sin b\cos l + V/r\sin b\sin l - W/r\cos b + \omega_1\sin l - \omega_2\cos l - \frac{1}{2}M_{12}^{+}\sin 2b\sin 2l + M_{13}^{+}\cos 2b\cos l + M_{23}^{+}\cos 2b\sin l - \frac{1}{4}M_{11}^{*}\sin 2b\cos^2 l + \frac{1}{2}X\sin 2b. \quad (6)$$

Equations (5) and (6) are often used for the simultaneous solution based on the total proper motions from some catalogue. In this case, if the distances to stars are unknown or known not accurately enough, then $U/\langle r\rangle$, $V/\langle r\rangle$, and $W/\langle r\rangle$, where $\langle r\rangle$ is the mean distance of the sample of stars for which the solution is obtained, are determined instead of U, V, and W.

Tables 1 and 2 present the simultaneous solution for Gaia EDR3 stars, while the plots in Figs. 1–3 illustrate the data from the tables.

An analysis of these result shows that the solar terms $U/\langle r\rangle$, $V/\langle r\rangle$, $W/\langle r\rangle$, as expected, decrease with increasing magnitude, because there is a close correlation between the stellar brightness and distance. The largest component is the one along the Y axis, $V/\langle r\rangle$. For bright stars of magnitudes 3, 4, 5, and 6 these parameters are determined unreliably; the same is also true for all of the remaining parameters. The reason for this is not only a small number of stars in this range (it is nevertheless not that small for equations with 11 parameters), but also peculiar kinematics of nearby stars. Researchers drew attention to this fact already since the 1950s (Shatsova 1950).

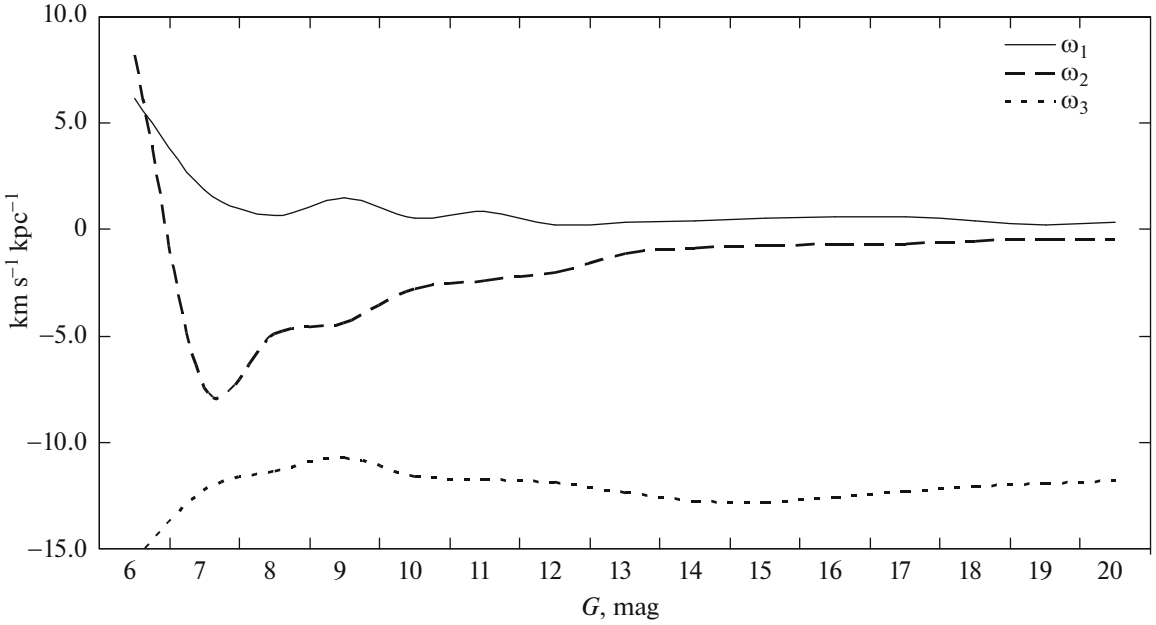

Fig. 2. Angular velocity of rigid-body rotation ω_1, ω_2, ω_3 (km s^{-1}kpc^{-1}) versus magnitude.

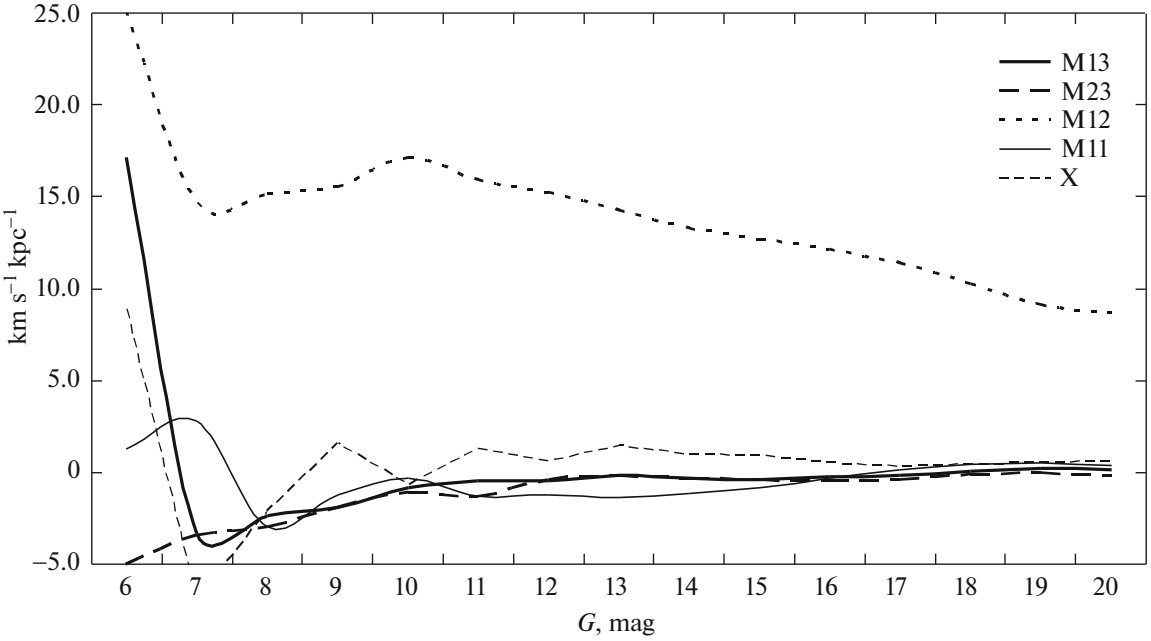

Fig. 3. Deformation tensor components M_{12}^{+}, M_{13}^{+}, M_{23}^{+}, M_{11}^{+}, X (km s^{-1}kpc^{-1}) versus magnitude.

Considering such an important parameter as the angular velocity of rigid-body rotation of the system (ω_1, ω_2, ω_3), we also see that the parameters of the angular velocity vector for the brightest stars cannot be determined at all, while beginning from stars of magnitude 7, the vector is well determined and is not perpendicular to the Galactic plane; this fact is also known (Tsvetkov and Amosov 2019). The following circumstances are interesting. First, beginning from stars of magnitude 12, the errors in the parameters being determined become very small. The smallness of the errors implies that the stars ideally obey the adopted model and do not contain any other kinematic components, but we will see that this is not quite the case. Second, the angular velocity components ω_1 and ω_2 differ significantly from zero even for

Table 3. The components of the solar motion, in km s^{-1}, and the angular velocity of rigid-body rotation, in km s^{-1} kpc^{-1}, derived from the simultaneous solution for stars at various distances

r	U	V	W	ω_1	ω_2	ω_3
0–100	10.2 ± 0.1	22.0 ± 0.1	7.2 ± 0.1	-1.1 ± 1.4	-12.1 ± 1.4	-1.5 ± 1.4
100–200	9.7 ± 0.0	23.2 ± 0.0	7.3 ± 0.0	1.2 ± 0.2	-6.3 ± 0.2	-10.1 ± 0.2
200–300	9.9 ± 0.0	24.7 ± 0.0	7.7 ± 0.0	1.1 ± 0.1	-2.5 ± 0.1	-12.5 ± 0.1
300–400	10.3 ± 0.0	25.8 ± 0.0	7.8 ± 0.0	0.8 ± 0.1	-1.3 ± 0.1	-13.0 ± 0.1
500–600	10.8 ± 0.0	27.7 ± 0.0	7.8 ± 0.0	1.0 ± 0.0	-1.1 ± 0.0	-13.7 ± 0.0
700–800	11.5 ± 0.0	30.7 ± 0.0	7.8 ± 0.0	-0.1 ± 0.0	-0.4 ± 0.0	-13.7 ± 0.0
900–1 K	12.1 ± 0.0	34.6 ± 0.0	8.0 ± 0.0	0.1 ± 0.0	0.2 ± 0.0	-13.7 ± 0.0
1.2–1.3 K	2.9 ± 0.1	40.5 ± 0.1	8.0 ± 0.1	0.7 ± 0.0	0.5 ± 0.0	-13.8 ± 0.0
1.5–1.6 K	13.4 ± 0.1	46.5 ± 0.1	8.1 ± 0.1	1.2 ± 0.1	0.4 ± 0.1	-14.0 ± 0.1
1.8–1.9 K	13.4 ± 0.1	52.4 ± 0.1	8.0 ± 0.1	1.2 ± 0.1	0.4 ± 0.1	-14.2 ± 0.1
2.1–2.2	13.5 ± 0.2	58.2 ± 0.2	8.0 ± 0.2	1.2 ± 0.1	0.3 ± 0.1	-14.5 ± 0.1
2.4–2.5	13.9 ± 0.2	62.2 ± 0.2	7.8 ± 0.2	0.0 ± 0.1	0.0 ± 0.1	-14.9 ± 0.1

Table 4. The deformation tensor components, in km s^{-1} kpc^{-1}, derived from the simultaneous solution for stars at various distances and the number of stars involved in the solution

G	M_{12}^{+}	M_{13}^{+}	M_{23}^{+}	M_{11}^{*}	X	N
0–100	28.0 ± 1.8	4.2 ± 1.8	-2.4 ± 1.8	-1.7 ± 3.6	0.1 ± 3.6	372 226
100–200	19.4 ± 0.3	-1.3 ± 0.3	-1.2 ± 0.3	-2.3 ± 0.5	0.1 ± 0.5	1 862 090
200–300	15.7 ± 0.1	-0.7 ± 0.1	-0.8 ± 0.1	-5.1 ± 0.2	1.6 ± 0.2	3 515 477
300–400	14.7 ± 0.1	-0.5 ± 0.1	-0.3 ± 0.1	-5.9 ± 0.2	2.2 ± 0.1	4 696 935
500–600	14.5 ± 0.1	-1.1 ± 0.1	-0.6 ± 0.1	-6.5 ± 0.1	2.1 ± 0.1	5 245 459
700–800	14.1 ± 0.1	-0.4 ± 0.1	0.8 ± 0.1	-5.3 ± 0.1	2.1 ± 0.1	5 272 993
900–1 K	13.5 ± 0.1	-0.1 ± 0.1	0.3 ± 0.1	-4.1 ± 0.1	1.8 ± 0.1	5 235 217
1.2–1.3 K	12.8 ± 0.1	-0.1 ± 0.1	-0.6 ± 0.1	-3.4 ± 0.1	1.2 ± 0.1	4 741 504
1.5–1.6 K	12.4 ± 0.1	-0.2 ± 0.1	-1.1 ± 0.1	-3.0 ± 0.1	1.4 ± 0.1	3 871 940
1.8–1.9 K	11.8 ± 0.1	-0.3 ± 0.1	-1.2 ± 0.1	-2.8 ± 0.2	1.4 ± 0.1	2 839 861
2.1–2.2	11.1 ± 0.1	-0.4 ± 0.1	-1.2 ± 0.1	-2.5 ± 0.2	1.2 ± 0.1	1 655 812
2.4–2.5	10.3 ± 0.1	-0.7 ± 0.1	-0.5 ± 0.1	-2.4 ± 0.2	1.2 ± 0.2	1 041 495

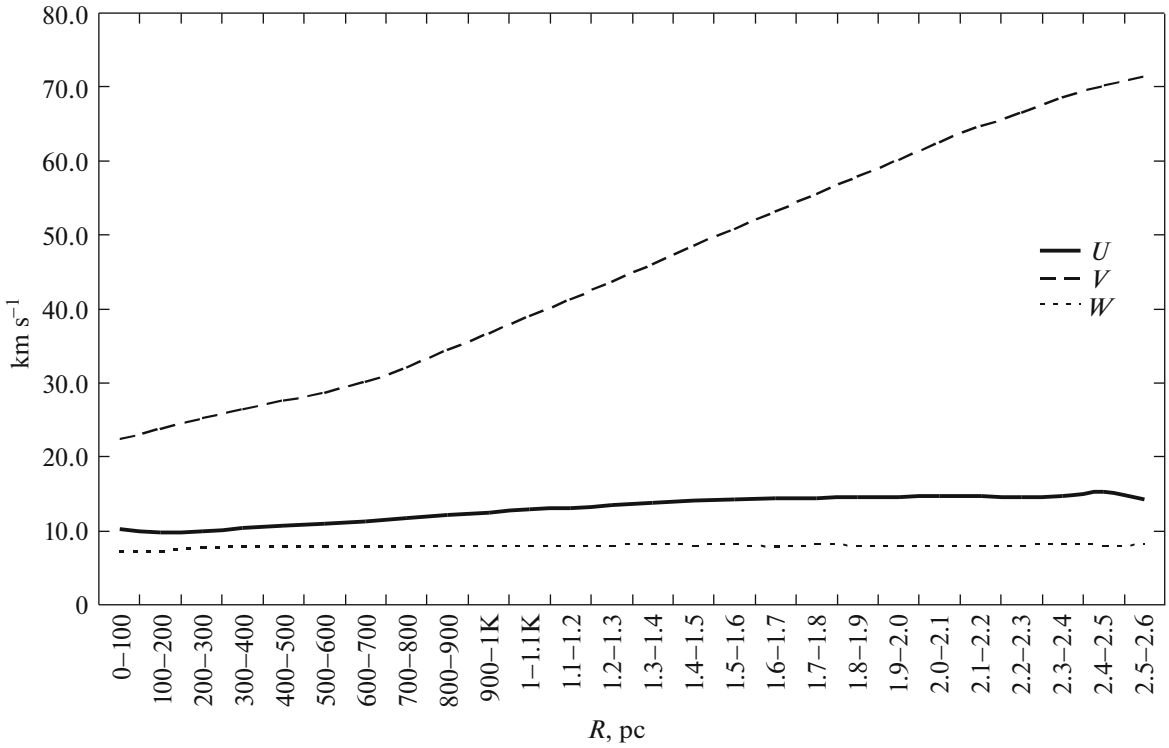

Fig. 4. Kinematic parameters of the solar motion U, V, W (km s^{-1}) versus distance to stars.

faint (and apparently distant) stars, suggesting that the angular velocity vector is not quite perpendicular to the Galactic plane.

An analysis of the deformation tensor components shows that almost all of the components, except for M_{12}^{+} (and this is the Oort parameter A), decrease rapidly toward zero values. A slight exception is the parameter M_{11}^{+} responsible for the difference of the stellar system's extensions along the X and Y axes. It retains a nonzero value for quite a long time and decreases noticeably only for stars of magnitudes 16–17 or fainter.

KINEMATICS OF STARS WITH A PARALLAX ACCURACY BETTER THAN 10%

An analysis of the distributions of stars in parallaxes and their accuracies shows that stars with a high relative parallax accuracy should be used for the stellar-kinematics studies that need the distances. For this purpose, we produced a sub-catalogue consisting of 98 506 335 stars that satisfy this criterion. Since even the formal 10% parallax accuracy does not yet guarantee a reliable parallax for each star, we proceeded in a standard way by dividing the stellar material into spherical layers located at different distances from the Sun. For these groups of stars we solved the equations within the Ogorodnikov–Milne model and decomposed the proper motions into a system of vector spherical harmonics. The results are presented in Tables 3 and 4. For compactness, beginning from 400 pc, the results are presented not in succession, because the values change slowly. The number of stars used in the solution is additionally given in Table 4. The solution itself was based on the proper motion and distance data averaged over 49 152 HealPix fields ($N = 64$) with equal field weights. Figures 4–6 illustrate the content of Tables 3 and 4.

An analysis of the results shows that the three-dimensional model is able to satisfactorily describe the stellar kinematics within 1.5–2 kpc, although the parameters themselves sometimes undergo significant changes, depending on the group of stars under consideration (especially the solar parameter V). As before, the nearest stars constitute a problem region where the kinematics does not obey the three-dimensional model. However, from a distance $\sim$300 pc the kinematic parameters take their usual values. Stars within 100 pc of the Sun have high peculiar velocities that simply cease to be noticeable with increasing distance, because the global Galactic rotation effects grow.

Generally speaking, it is believed that the simplified linear Oort–Lindblad model or the complete Ogorodnikov–Milne model can be used up to distances of 1–1.5 kpc (Ogorodnikov 1965). However, we see that the Oort parameters $A = M_{12}$ and $B =$

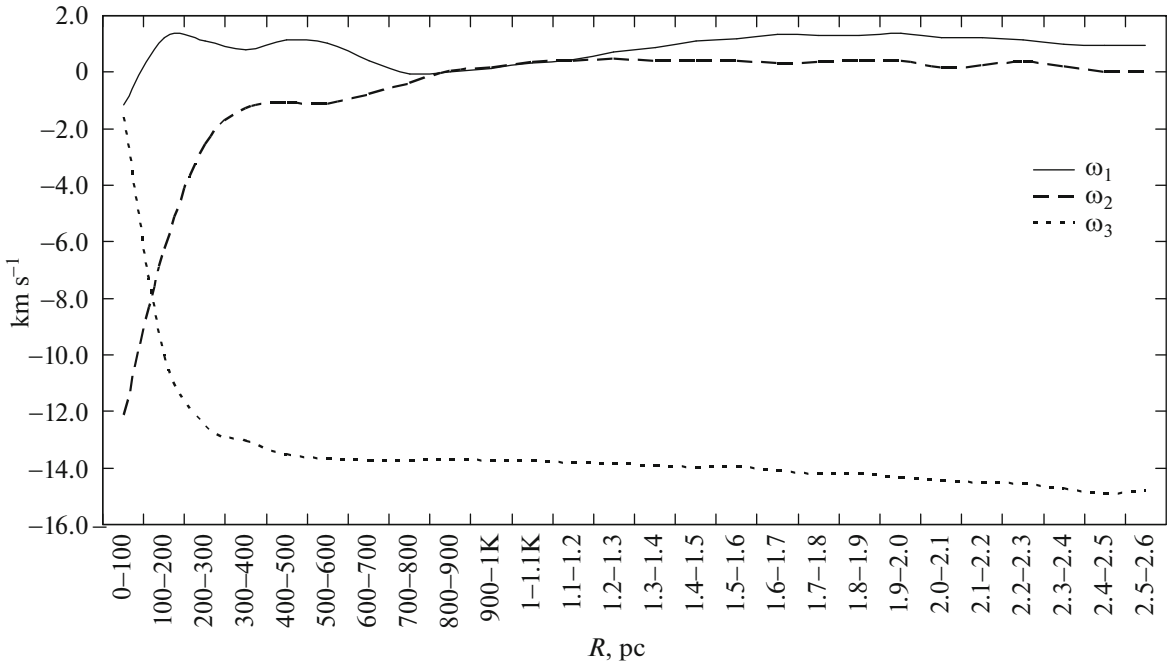

Fig. 5. Angular velocity of rigid-body rotation $\omega_1, \omega_2, \omega_3$ (km s^{-1} kpc^{-1}) versus distance to stars.

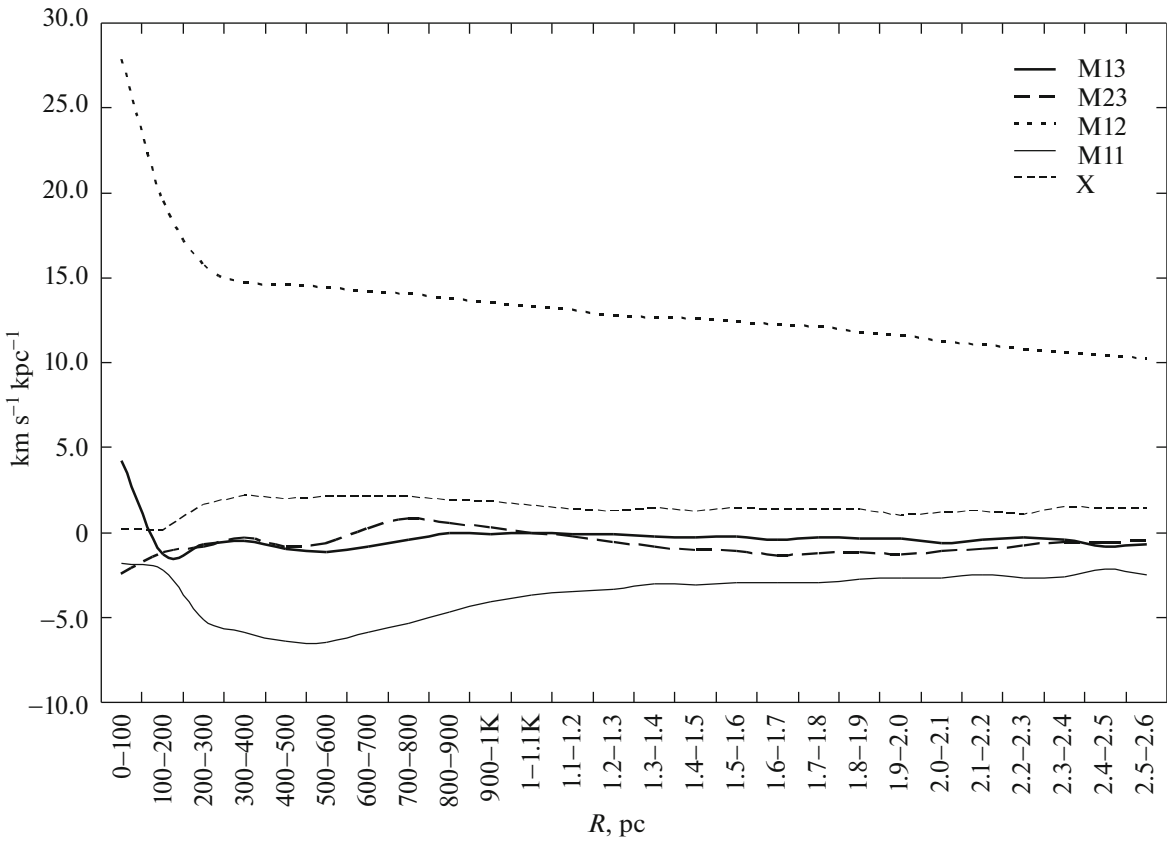

Fig. 6. Deformation tensor components M_{13}^{+}, M_{23}^{+}, M_{11}^{+}, X (km s^{-1} kpc^{-1}) versus the distance to stars.

ω_3 change with distance, though very gradually, retaining their overall pattern. The other parameters (the components of the angular velocity ω_1 and ω_2 and the deformation tensor M^*_{11}, M^+_{13}, M^+_{23}, X) tend to nearly zero values with increasing distance. Possibly only M^*_{11} shows nonzero values (the difference of the system's contractions along the X and Y axes).

The behavior of the parameter V, the solar velocity along the Y axis, i.e., along the axis in the direction of Galactic rotation, is most striking. Obviously, the explanation can be as follows: the solar velocity is estimated relative to the groups of stars at different distances, and these groups move themselves relative to one another. These differences are great and have a large systematic trend in the Galactic plane in a direction perpendicular to the one toward the Galactic center. Previously, we obtained similar results based on the Gaia DR2 with RV catalogue (Tsvetkov and Amosov 2019), but the behavior of the parameter V was slightly different. Its value remained stable (about 22 km s^{-1}) up to a distance of 800 pc and, further out, a linear increase began. In our case, we observe a linear increase immediately.

Another peculiarity of the solar motion parameters is their reliable and predictable values even for the nearest stars, which cannot be said about the rotation and deformation parameters that reach stable values only from distances of 400–500 pc.

CONCLUSIONS

Our results are in good agreement with the data of other researchers based on the material of previous versions of the Gaia catalogues (Bovy 2017; Velichko et al., 2020). We showed that the solar motion parameters U and W, all three angular velocity components, and the deformation tensor components M^+_{13}, M^+_{23}, M^*_{11}, X are relatively constant at distances greater than 500 pc. A systematic trend with distance is clearly observed for the component V and the Oort parameter $A = M^+_{12}$. The change in these parameters stems from the fact that the behavior of the angular velocity of Galactic rotation in the center–anticenter direction is nonlinear. Our next paper will be devoted to the construction of such a model and its detailed analysis. In addition, the completeness of the Ogorodnikov–Milne model remains in question. Our previous studies based on the material of the previous Gaia DR2 release (Tsvetkov et al. 2020) show the presence of systematic components in the proper motions that are not described by this model. This question will also be discussed in our next paper.

REFERENCES

1. O. V. Bartentiev, *Modern Fortran,* 3rd ed. (DIALOG MIFI, Moscow, 2000) [in Russian].
2. Jo Bovy, Mon. Not. R. Astron. Soc. Lett. **468**, L63 (2017).
3. A. Brown, A. Vallenari, T. Prusti, et al., Astron. Astrophys. **649** (2021).
4. L. Casagrande and D. van den Berg, Mon. Not. R. Astron. Soc. Lett. **479**, L102 (2018).
5. ESA Gaia. https://sci.esa.int/web/gaia.
6. Gaia Collab., Astron. Astrophys. **649**, A1 (2021).
7. Gaia, EDR3. https://www.cosmos.esa.int/web/gaia/earlydr3.
8. Gaia, Chapter 13. https://gea.esac.esa.int/archive/documentation/GEDR3/Gaia_archive/chap_datamodel/.
9. K. M. Gorski, E. Hivon, A. J. Banday, et al., Astrophys. J. **622**, 759 (2005).
10. H. L. Johnson and W. W. Morgan, Astrophys. J. **117**, 313 (1953).
11. D. Katz et al., Astron. Astrophys. **622**, A205 (2019).
12. D. Michalik, L. Lindegren, and D. Hobbs, Astron. Astrophys. **574**, A115 (2015).
13. B. A. du Mont, Astron. Astrophys. **61**, 127 (1977).
14. P. Montegriffo, F. de Angeli, M. Bellazzini, et al., Gaia EDR3 passbands. https://www.cosmos.esa.int/web/gaia/edr3-passbands. Accessed 2020.
15. K. F. Ogorodnikov, *Dynamics of Stellar Systems* (Fizmatgiz, Moscow, 1965) [in Russian].
16. M. Riello, F. de Angeli, D. W. Evans, et al., Astron. Astrophys. **649**, A3 (2021).
17. S. Roeser, M. Demleitner, and E. Schilbach, Astron. J. **139**, 2440 (2010).
18. S. P. Rybka, Kinem. Fiz. Nebesn. Tel **20**, 437 (2004).
19. R. B. Shatsova, Uch. Zap. LGU, №136 (1950).
20. A. S. Tsvetkov, *Guide for Practical Work with the Hipparcos Catalogue* (St. Petersburg, 2005) [in Russian].
21. A. S. Tsvetkov and F. A. Amosov, Astron. Lett. **45**, 462 (2019).
22. A. S. Tsvetkov, F. A. Amosov, D. A. Trofimov, and S. D. Petrov, Astron. Lett. **46**, 58 (2020).
23. A. Velichko, P. Fedorov, and V. Akhmetov, Mon. Not. R. Astron. Soc. **494**, 1430 (2020).
24. V. V. Vityazev and A. S. Tsvetkov, Mon. Not. R. Astron. Soc. **442**, 1249 (2014).
25. V. V. Vityazev, A. V. Popov, A. S. Tsvetkov, S. D. Petrov, D. A. Trofimov, and V. I. Kiyaev, Astron. Lett. **44**, 236 (2018).
26. V. V. Vityazev, A. S. Tsvetkov, V. V. Bobylev, and A. T. Bajkova, Astrophysics **60**, 503 (2017).
27. N. Zacharias, D. G. Monet, S. E. Levine, et al., Bull. Am. Astron. Soc. **36**, 1418 (2004).

Translated by N. Samus'